Open Access

OBM Genetics

LIDSEN Publishing Inc.

Case Report

Clinical and Molecular Cytogenetic Characterization of a *De Novo* 3q26.33-q28 Duplication: Case Report and Literature Review

Hicham Bouchahta [1, 2], Nada Benyahya [3], Zhour EL Amrani [2, 4], Fatima Oubouksss [3], Thomas Liehr [5], Siham Chafai Elalaoui [2, 4], Isabel Marques Carreira [6], Yassamine Doubaj [2], Abdelhafid Natiq [4, 7, *], Laila Sbabou [1]

1. Microbiology and Molecular Biology Team, Center of Plant and Microbial Biotechnology, Biodiversity and Environment, Faculty of Sciences, Mohammed V University in Rabat, Avenue Ibn Battouta, BP 1014, Rabat 10000, Morocco; E-Mails: tech.bouchahta@gmail.com; l.sbabou@um5r.ac.ma
2. Department of Medical Genetics, National Institute of Health in Rabat, BP 769 Agdal, Rabat 10090, Morocco; E-Mails: zhourel31@gmail.com; elalaoui.sc@gmail.com; y1doubaj@gmail.com
3. Medical Genetics Unit, Children's Hospital, Ibn Sina University Hospital Center (CHU Ibn Sina), Faculty of Medicine and Pharmacy, Mohammed V University, Rabat, Morocco; E-Mails: nada.ben4894@gmail.com; fatimaoubouksss@gmail.com
4. Research team in genomics and molecular epidemiology of genetic diseases, Genomics Center of Human Pathologies, Faculty of Medicine and Pharmacy, University Mohammed V in Rabat, Morocco; E-Mails: a.natiq@um5r.ac.ma; abdelnat@yahoo.fr
5. Jena University Hospital, Friedrich Schiller University, Institute of Human Genetics, Jena, Germany; E-Mail: Thomas.Liehr@med.uni-jena.de
6. Coimbra Institute for Clinical and Biomedical Research (iCBR) and Center of Investigation on Environment Genetics and Oncobiology (CIMAGO), Faculty of Medicine, University of Coimbra,3000-548 Coimbra, Portugal; E-Mail: icarreira@fmed.uc.pt
7. National Laboratory Mohammed VI UM6SS, Casablanca, Morocco

* **Correspondence:** Abdelhafid Natiq; E-Mails: a.natiq@um5r.ac.ma; abdelnat@yahoo.fr

Academic Editor: Ivan Y Iourov

Collection: Applications of Fluorescence in Situ Hybridization II.

OBM Genetics
2026, volume 10, issue 2
doi:10.21926/obm.genet.2602341

Received: February 06, 2026
Accepted: May 13, 2026
Published: May 19, 2026

Abstract

Isolated duplications of the long arm of chromosome 3 (3q) are rare chromosomal abnormalities. To date, approximately 32 pure cases have been documented. Most reported 3q duplications arise from unbalanced translocations or inversion-loops mechanisms and are associated with additional chromosomal imbalances, making pure duplications particularly valuable for genotype-phenotype correlations. We report a 17-year-old female with a *de novo* pure tandem duplication of 3q26.33-q28 (~10.945 Mb). The clinical course was marked by neonatal distress with hypotonia, severe global developmental delay (independent walking at 24 months, language acquisition at 4 years), intellectual disability, autism spectrum disorder, and epilepsy. Dysmorphic features included esotropia, thin upper lip, high arched eyebrows, flat occiput, short neck, and generalized hirsutism. Notably, the patient exhibited increased birth weight (4000 g), contrasting with the growth retardation commonly described in 3q duplication syndrome, and no congenital cardiac anomalies were detected. Conventional R-banded karyotyping, fluorescence in situ hybridization (FISH), and chromosomal microarray analysis (CMA) were performed on peripheral blood samples from the patient and both parents. Karyotype analysis revealed 46, XX, add(3)(q?). CMA identified a duplication defined as arr[GRCh37] 3q26.33q28(179,659,847_190,604,567) × 3. FISH analysis confirmed the tandem configuration of the duplicated segment. Parental karyotypes were normal, supporting a *de novo* origin of the rearrangement. The duplicated region encompasses 31 OMIM morbid genes, including *SOX2*, *IGF2BP2* and *TP63*. This case represents the first reported pure 3q duplication since a 2023 comprehensive review, which documented 31 cases. The phenotypic profile suggests region-specific contributions to the 3q duplication syndrome phenotype. This case provides a refined genotype-phenotype correlation and underscores the diagnostic value of an integrated cytogenetic approach combining conventional and molecular techniques.

Keywords

Chromosome 3q duplication; partial trisomy 3q; duplication 3q26.33-q28; conventional cytogenetic banding; molecular cytogenetics; chromosomal microarray analysis; developmental delay; dysmorphic features

1. Introduction

Partial trisomy of the long arm of chromosome 3 (=3q), first described in 1966 [1], is a well-defined clinical entity. The most frequent clinical manifestations include characteristic facial dysmorphism, such as microcephaly and low-set ears, malformations of the hands and feet, hirsutism, congenital heart defects, and growth and psychomotor retardation [2]. Cases with isolated duplication of 3q are rare; in most cases, 3q duplications are associated with a partial monosomy of another autosomal region, often resulting from an unbalanced parental translocation. Accordingly, approximately 70% of such cases are inherited from a balanced translocation [3]. To date, 32 cases of pure partial 3q duplications with different breakpoints along the long arm of chromosome 3 have been described in the literature [3-7]. Since the comprehensive review by Serra

et al. [3] in 2023, no additional pure 3q duplication cases have been published. The present case therefore represents the first documented case of pure 3q duplication since that review, further contributing to the limited body of literature on this rare chromosomal abnormality.

Cases presenting with isolated 3q duplications are particularly valuable for delineating the phenotypic spectrum associated with this chromosomal imbalance. Here, we describe a 17-year-old female carrying a *de novo* duplication of the 3q26.33-q28 region (~10.9 Mb), identified by chromosomal microarray analysis (CMA) and subsequently confirmed by fluorescence in situ hybridization (FISH).

1.1 Case Presentation

The patient is a 17-year-old female referred to the Department of Medical Genetics in Rabat for the evaluation of psychomotor delay, delayed acquisition of independent walking (started walking at 2 years), and facial dysmorphism. She is the second child of healthy, non-consanguineous parents with maternal age 28 years and paternal age 32 years at the time of delivery. There was no family history of congenital anomalies, intellectual disability, genetic disorders, recurrent miscarriages, or any other significant medical conditions.

She was delivered by cesarean section at 38 weeks of gestation, with a birth weight of 4000 g. The neonatal period was marked by distress with delayed crying and generalized hypotonia. Developmental milestones were globally delayed: independent sitting was achieved at 12 months, independent walking at 24 months, and expressive language acquisition at approximately 4 years of age. Throughout childhood, she exhibited persistent learning difficulties, resulting in repeated academic years. Neurodevelopmental assessment revealed language impairment, hypoactivity, intellectual disability, and marked deficits in social interaction, with autistic traits including social withdrawal and self-injurious behavior.

At the age of 12 years, the patient was diagnosed with acute rheumatic fever following a streptococcal infection and has since been on long-term secondary prophylaxis with benzathine penicillin G. Her medical history also includes epilepsy; however, detailed seizure semiology and information regarding antiepileptic treatment were not available at the time of genetic evaluation.

At the time of clinical evaluation, her body weight was 52 kg. Physical examination revealed multiple dysmorphic features, including right convergent strabismus with decreased visual acuity on ophthalmologic assessment, high-arched eyebrows, a thin upper lip, a flat occiput, a short neck, generalized hirsutism, and thoracic kyphosis. Delayed closure of the anterior fontanelle was reported, with closure occurring before the age of 2 years.

Brain magnetic resonance imaging (MRI) showed lesions of presumed infectious origin in the right occipital region. Additional investigations including transthoracic echocardiography, abdominal and renal ultrasound were normal. The electroencephalogram (EEG) showed normal background activity.

2. Materials and Methods

2.1 Banding Cytogenetics

Written informed consent was obtained from the patient's parents before sample collection, in accordance with institutional ethical guidelines. Peripheral venous blood samples (3-5 mL) were

collected from the patient and both parents in heparinized tubes for cytogenetic and molecular cytogenetic analyses.

Chromosome analysis was performed on cultured peripheral blood lymphocytes from the proband and both parents using standard cell culture and R-banding techniques. Karyotypes were established and interpreted according to the recommendations of the International System for Human Cytogenomic Nomenclature (ISCN 2024).

2.2 Chromosomal Microarray Analysis

Genomic DNA was extracted from peripheral blood samples using a commercially available extraction kit, according to the manufacturer's instructions. CMA was performed using the Agilent 4 × 180 K ISCA v2 oligonucleotide microarray (25 kb median probe spacing). Hybridization, washing, and scanning procedures were performed according to the manufacturer's protocols.

Microarray data were analyzed with Agilent Cytogenomics software (version 2.9.2.4). Genomic coordinates were interpreted with reference to the human genome assembly GRCh37/hg19.

2.3 Molecular Cytogenetics Analysis

FISH was performed according to standard protocols using a panel of different probes: locus-specific probes RP11-510K16 in 3q26.33 (hg19: 180,170,578-180,373,271), RP11-110C15 in 3q27.2 (hg19: 185,131,537-185,285,430), RP11-95L3 in 3q28 (hg19: 190,397,346-190,547,833). In addition, a subtelomeric probe specific for 3qter (D3S4560, 3q29; Abbott/Vysis) was used.

2.4 Statement of Ethics

2.4.1 Study Approval Statement

The whole pre-analytic and post-analytic steps described in this work were performed for patients by the Department of Medical Genetics of the National Institute of Health as part of medical services, in accordance with the tenets of the Declaration of Helsinki.

All ethical issues were respected in accordance with the guidelines of the Intramural Advisory Committee of the Department of Medical Genetics, National Institute of Health, Rabat, Morocco.

2.4.2 Consent to Publish Statement

Written informed consent was obtained from the parents of the patient for publication of the details of their medical case and any accompanying images.

3. Results

Conventional chromosome analysis revealed normal karyotypes in both parents (Figure 1). In contrast, karyotyping of the proband identified an abnormal chromosome 3, 46, XX, add(3)(q?), indicating the presence of additional chromosomal material of unknown origin on the long arm of chromosome 3 (Figure 2).

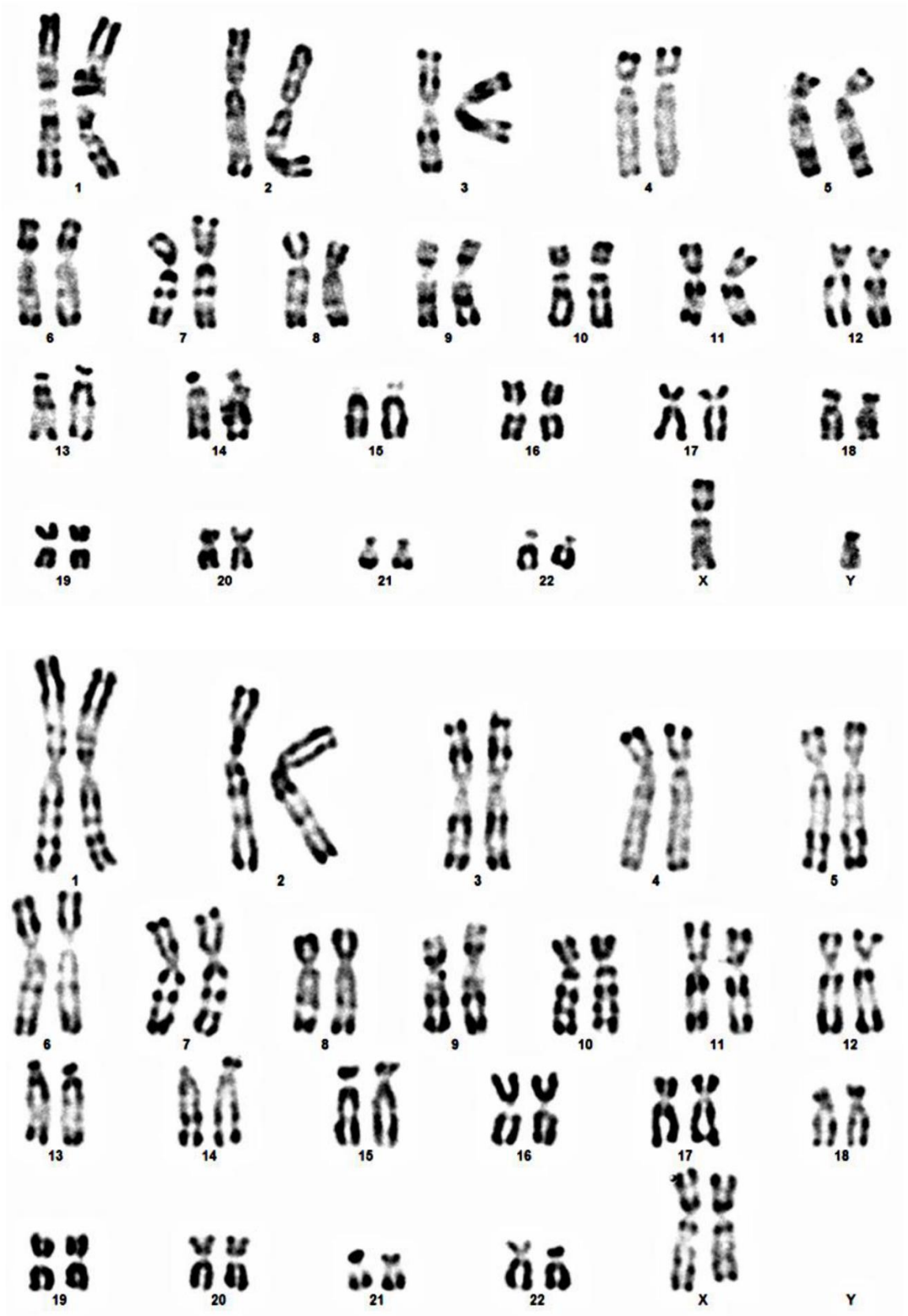

Figure 1 Normal R-banded karyotypes of the patient's parents.

Figure 2 R-banded karyotype of the patient showing an abnormal chromosome 3.

CMA revealed a female hybridization pattern showing a duplication on the long arm of chromosome 3, spanning genomic coordinates 179,659,847 bp to 190,604,567 bp (GRCh37), corresponding to the cytogenetic region 3q26.33-q28. This duplication was reported as arr[GRCh37] 3q26.33q28(179,659,847_190,604,567) × 3 (Figure 3).

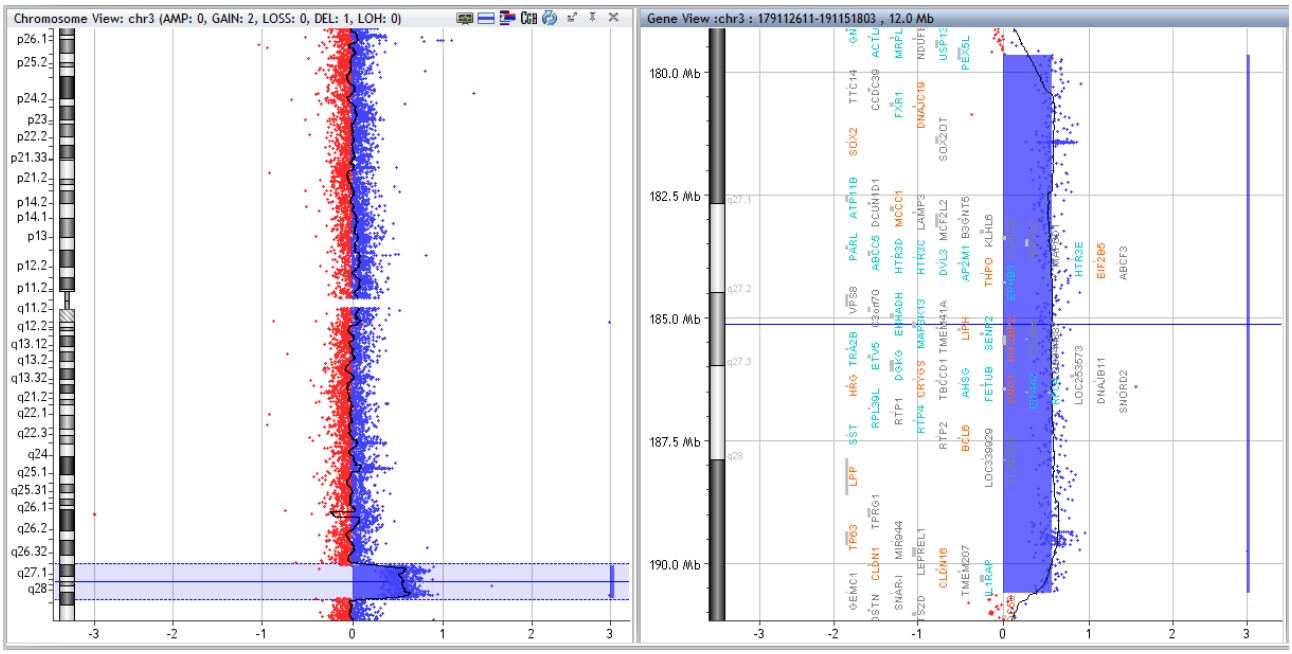

Figure 3 Chromosomal microarray analysis (CMA) results for the patient.

FISH analysis confirmed the presence of the duplicated segment on the derivative chromosome 3. The derivative chromosome 3 was therefore characterized as ish dup(3)(q26.33q28)(RP11-510K16+, RP11-110C15+, RP11-95L3+, RP11-510K16+, RP11-110C15+, RP11-95L3+, D3S4560+), consistent with a tandem duplication of the 3q26.33-q28 region (Figure 4).

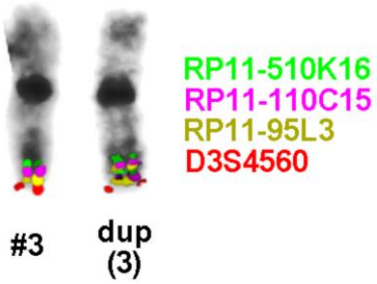

Figure 4 FISH analysis confirming the duplication of the 3q26.33-q28 region.

The duplicated region spans approximately 10.9 Mb and contains several genes involved in neurodevelopment, growth regulation, and morphogenesis. Figure 5 illustrates the duplicated genomic interval 3q26.33-q28, highlighting several OMIM morbid genes, including *SOX2*, *IGF2BP2*, and *TP63*, which may contribute to the patient's neurodevelopmental impairment and dysmorphic features.

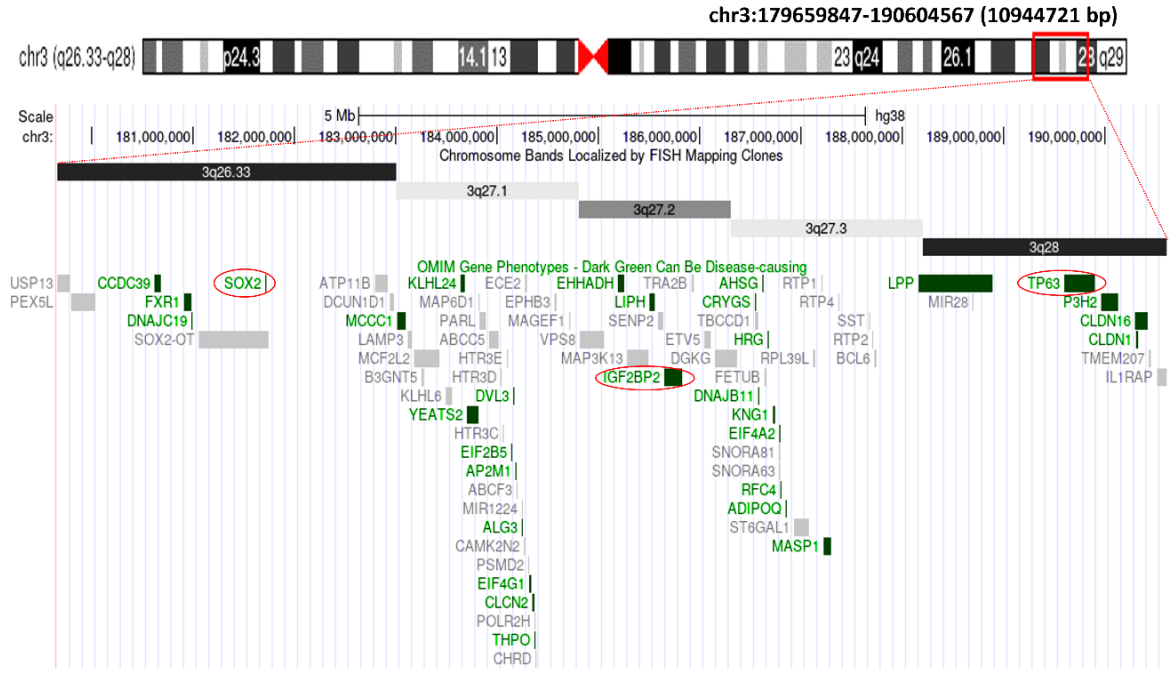

Figure 5 Schematic overview of the 3q26.33-q28 duplication and associated genes. Schematic representation of chromosome 3 illustrating the duplicated segment identified in our patient, spanning approximately 10.9 Mb (genomic coordinates 179,659,847-190,604,567 bp, according to the UCSC Genome Browser). OMIM genes are color-coded, with dark green indicates morbid genes with established clinical relevance and gray represents other OMIM genes. Genes highlighted with red circles correspond to those previously reported to be associated with intellectual disability within this region.

In summary, the patient carries a *de novo* partial trisomy 3q26.33q28, corresponding to genomic coordinates 3q26.33q28(179,659,847_190,604,567)(GRCh37).

4. Discussion

The minimal critical genomic region associated with the characteristic phenotype of 3q duplication syndrome was initially proposed to be limited to subband 3q26.3. Subsequent studies refined this critical interval to 3q26.3-3q27, while more recent reports extended it to 3q26.3-3q29. The clinical expression of 3q duplication syndrome is highly variable and largely depends on the size and precise breakpoints of the duplicated segment.

Despite this phenotypic heterogeneity, several recurrent clinical features have been consistently reported, including facial dysmorphism, hirsutism, microcephaly, intellectual disability, growth retardation, genitourinary anomalies, hands and feet malformations, as well as renal and congenital heart defects [2-7].

When comparing our patient's phenotype with previously reported cases of pure 3q duplications (Table 1, Figure 6), several overlapping clinical features were identified. The patient showed facial dysmorphism, including high arched eyebrows, a thin upper lip, and a flat occiput, as well as a short neck and generalized hirsutism. In addition, she exhibited severe neurodevelopmental involvement, characterized by global developmental delay, intellectual disability, and autistic features.

Table 1 Reported cases of pure 3q duplication: cytogenetic and clinical findings.

Case	Duplicated region	Size (Mb)	Methods	Key clinical features	Reference
1	3q24-q26.31	~30	Karyotype	**Craniofacial/Dysmorphic:** microcephaly, downslanting palpebral fissures, epicanthus, bulbous nasal tip, prominent philtrum, large or downturned corners of the mouth, low-set dysplastic ears **Neurological/Neurodevelopmental:** developmental delay **Growth:** Not reported **Cardiac:** heart defects **Limb/Skeletal:** Not reported **Genitourinary:** Not reported	Meins et al. 2005 [4]
2-3	3q25-29	~48	Karyotype	**Craniofacial/Dysmorphic:** microcephaly, low frontal hairline, wide nasal bridge, bulbous nasal tip, large or downturned corners of the mouth, hirsutism **Neurological/Neurodevelopmental:** developmental delay **Growth:** Not reported	Wilson et al. 1978 [5]

				Cardiac: Not reported **Limb/Skeletal:** V finger clinodactyly **Genitourinary:** Not reported	
4-11	3q29	~1.6	CMA, FISH	**Craniofacial/Dysmorphic:** microcephaly/macrocephaly, low frontal hairline, down slanting palpebral fissures, wide nasal bridge, large or downturned corners of the mouth **Neurological/Neurodevelopmental:** developmental delay **Growth:** Growth retardation **Cardiac:** heart defects **Limb/Skeletal:** Not reported **Genitourinary:** Not reported	Ballif et al. 2008, Lisi et al. 2008 [6, 7]
12-13	3q26.3	~28	Karyotype, FISH	**Craniofacial/Dysmorphic**: low/high frontal hairline, bushy eyebrows, down slanting palpebral fissures, wide nasal bridge, bulbous nasal tip, prominent philtrum, large or downturned corners of the mouth, low-set dysplastic ears, hirsutism **Neurological/Neurodevelopmental:** developmental delay **Growth:** Postnatal growth retardation **Cardiac:** heart defects **Limb/Skeletal:** Not reported **Genitourinary:** Not reported	Faas et al. 2002, Azar et al. 1999 [2, 8]
14-24	3q25-qter	~48	Karyotype, various	**Craniofacial/Dysmorphic**: microcephaly, low frontal hairline, hypertelorism, downslanting palpebral fissures, epicanthus, wide nasal bridge, bulbous nasal tip, prominent philtrum, large downturned corners of the mouth, low-set dysplastic ears, hirsutism **Neurological/Neurodevelopmental:** developmental delay **Growth:** Prenatal growth retardation **Cardiac:** heart defects **Limb/Skeletal:** V finger clinodactyly **Genitourinary:** urogenital anomalies	ECARUCA database

25-30	3q27-qter	~20	Karyotype, various	**Craniofacial/Dysmorphic:** hypertelorism, downslanting palpebral fissures, epicanthus, wide nasal bridge, bulbous nasal tip, low-set dysplastic ears, hirsutism **Neurological/Neurodevelopmental:** developmental delay **Growth:** Prenatal growth retardation **Cardiac:** Not reported **Limb/Skeletal:** V finger clinodactyly **Genitourinary:** urogenital anomalies	ECARUCA database
31	3q26.32-q28	14.7	Karyotype, CMA, FISH	**Craniofacial/Dysmorphic:** hypertrichosis, facial dysmorphism (synophrys, epicanthic folds, thickened upper and lower lips, pointed chin, short neck, low-set ears), anisocoria **Neurological/Neurodevelopmental:** mild intellectual disability (IQ 68), mild speech delay, stereotypic movements, joint laxity, widened thoracic duct. **Growth:** Tall stature (birth weight 4250g at 90th percentile, maintained at 2 and 4 years) **Cardiac:** NO cardiac anomalies **Limb/Skeletal:** short hands with clinodactyly and deep furrows, short feet with dystrophic nails on halluces **Genitourinary:** Not reported	Pavone et al. 2016 [9]
32	3q27.1-q29	10.9	Karyotype, NIPT, a-CGH, FISH	**Craniofacial/Dysmorphic:** macrocephaly, low/high frontal hairline, bushy eyebrows, hypertelorism, down slanting palpebral fissures, epicanthus, wide nasal bridge, bulbous nasal tip, prominent philtrum, large or downturned corners of the mouth, low-set dysplastic ears, esotropia **Neurological/Neurodevelopmental:** mild motor delay, ASD **Growth:** Prenatal and postnatal overgrowth **Cardiac:** heart defects	Serra et al. 2023 [3]

				Limb/Skeletal: brachydactyly, V finger clinodactyly, hallux varus **Genitourinary:** hydronephrosis **Other:** hepatomegaly	
33 (Present case)	3q26.33-q28	10.9	Karyotype, CMA, FISH	**Craniofacial/Dysmorphic:** right convergent strabismus with decreased visual acuity, high arched eyebrows, thin upper lip, flat occiput, short neck, generalized hirsutism, delayed anterior fontanelle closure **Neurological/Neurodevelopmental:** neonatal distress with delayed crying and hypotonia, severe psychomotor delay (sitting at 1 year, walking at 2 years, language at 4 years), intellectual disability, autistic traits with social withdrawal and self-injurious behavior, epilepsy, learning difficulties with multiple grade repetitions, normal EEG background activity **Growth:** increased birth weight (4 kg at 38 weeks), current weight 52 kg **Cardiac:** NO cardiac anomalies (normal echocardiography) **Limb/Skeletal:** thoracic kyphosis **Genitourinary:** normal renal ultrasound **Other:** normal abdominal ultrasound, acute rheumatic fever (on benzathine penicillin G since age 12)	This report

Note: This table includes only pure 3q duplications without associated deletions or unbalanced translocations.

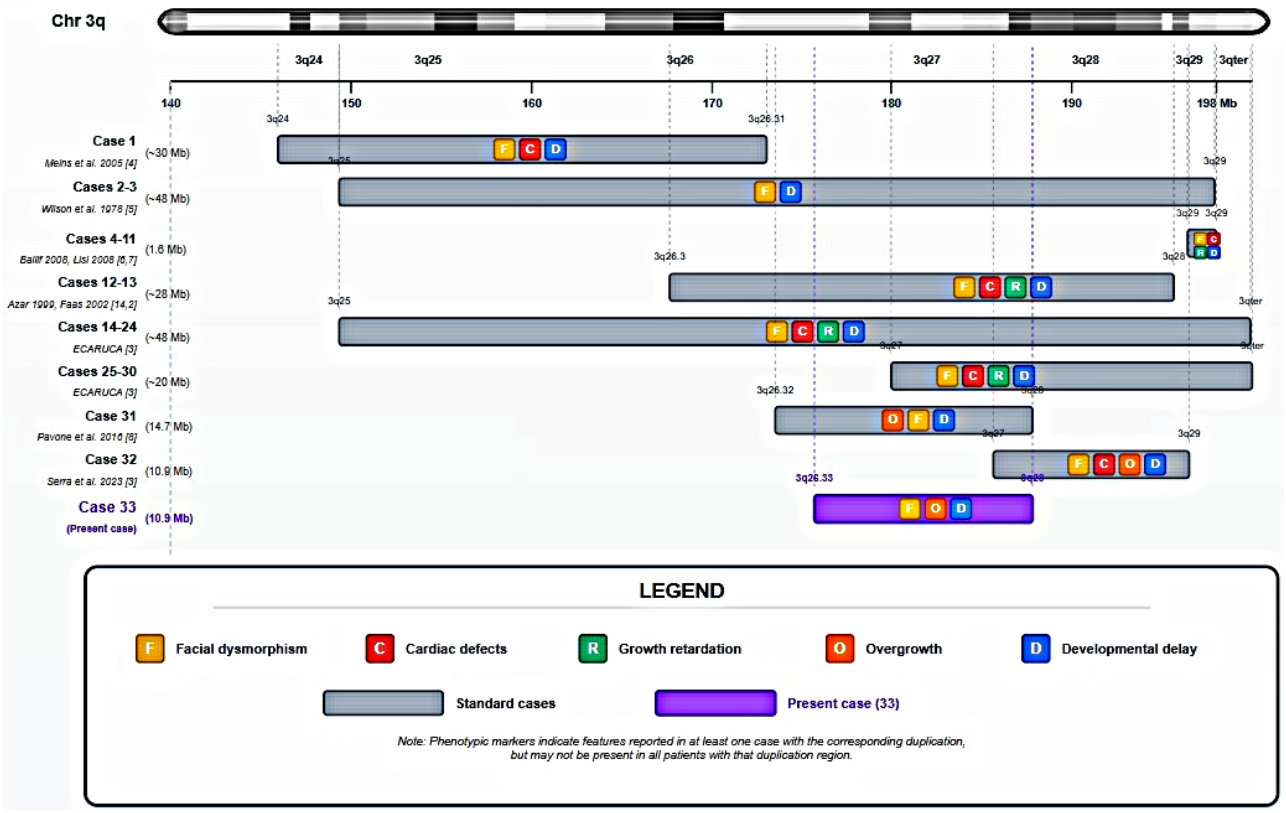

Figure 6 Comparative genomic mapping and phenotypic spectrum of reported pure 3q duplications.

Notably, no congenital cardiac malformations were identified in our patient. Cardiac involvement in 3q duplication syndrome shows considerable variability, with congenital heart defects reported in approximately 46% (6/13) of cases included in an early literature review. Nearly one-third of affected individuals do not survive beyond the first year of life, with mortality largely attributed to severe cardiac malformations and recurrent infections [2].

The duplicated segment identified in our patient (3q26.33-q28; chr3:179,659,847-190,604,567, GRCh37) is more distal than the initially defined critical region (3q26.3-q27.3), yet the patient exhibits most of the characteristic features of the 3q duplication syndrome. This observation suggests that key dosage-sensitive genes contributing to the core phenotype extend beyond the originally defined critical region into the 3q27-q28 interval.

The duplicated region encompasses hundreds of protein-coding genes, of which 31 are listed in the OMIM Morbid Map (Figure 5). To assess the functional impact of increased gene dosage, we evaluated the probability of triplosensitivity (pTriplo) for each of these 31 genes using the dosage sensitivity map. Three genes exceeded the high-confidence triplosensitivity threshold of pTriplo ≥ 0.94: *TP63* (pTriplo = 1.00), *AP2M1* (pTriplo = 0.99), and *EIF4G1* (pTriplo = 0.98). Several additional genes showed intermediate scores, including *FXR1* (0.90), *DVL3* (0.86), *YEATS2* (0.86), *IGF2BP2* (0.81), and *SOX2* (0.80), suggesting a broader dosage-sensitive landscape within this region. Among these, *SOX2* (3q26.33), highly expressed during embryonic and fetal brain development, plays a crucial role in maintaining neural progenitor cells and promoting neuronal differentiation [10]. The severe intellectual disability, epilepsy, and autistic features observed in our patient may therefore be partially explained by increased dosage of *SOX2* and other neurodevelopmentally relevant genes

within this interval. *TP63* (3q28), which achieved the highest pTriplo score of 1.00, is critical for limb and ectodermal development and may contribute to the ectodermal anomalies reported in some cases of 3q duplication [11]. *AP2M1* and *EIF4G1*, both with pTriplo scores exceeding 0.98, encode proteins involved in intracellular trafficking and translational regulation, respectively, and their triplosensitivity may further modulate the neurodevelopmental phenotype.

Our patient exhibited increased birth weight (4000 g at 38 weeks of gestation), in contrast to the growth retardation reported in approximately 61.5% of patients with pure 3q duplications [3, 5, 9]. The biological basis of this overgrowth phenotype remains incompletely understood. *IGF2BP2* (3q27.2), a member of the insulin-like growth factor 2 mRNA-binding protein family involved in prenatal and postnatal growth regulation, has previously been proposed as a candidate gene. However, its intermediate triplosensitivity score (pTriplo = 0.81), below the high-confidence threshold of 0.94 defined by Collins et al. [12], argues against a straightforward dosage-sensitive mechanism. Furthermore, cases 25-30 from the ECARUCA database (3q27-qter), whose duplication encompasses *IGF2BP2,* also presented with prenatal growth retardation, further challenging the hypothesis of *IGF2BP2* as the sole determinant of growth outcome. These observations suggest that the overgrowth phenotype observed in our patient reflects a complex interplay of multiple dosage-sensitive genes within the 3q26.33-q28 interval, potentially modulated by epigenetic factors or genes acting in trans.

A more informative approach to genotype-phenotype correlation emerges from comparing cases with near-identical duplication boundaries. The case reported by Pavone et al. [9], with a 3q26.32-q28 duplication, represents the closest genomic comparator to our patient (3q26.33-q28). Both cases share elevated birth weight, postnatal overgrowth, absence of congenital cardiac anomalies, generalized hirsutism, facial dysmorphism, and intellectual disability, a striking phenotypic convergence that supports a direct contribution of the 3q26.33-q28 interval to these features. Serra et al. [3], reporting a 3q27.1-q29 duplication, also described overgrowth, further supporting the association of the distal 3q27 region with growth excess in selected cases.

A more consistent genotype-phenotype correlation emerges for cardiac and genitourinary involvement. Neither our patient nor Pavone et al. presented with cardiac defects or genitourinary anomalies, whereas Serra et al. and cases 14-24 (ECARUCA, 3q25-qter), both extending beyond 3q28, exhibited cardiac defects and urogenital anomalies. This pattern suggests that genes responsible for cardiac and genitourinary involvement reside in the more distal 3q28-q29 interval, beyond our patient's duplication boundaries. However, as cardiac findings were not reported for cases 25-30 (ECARUCA, 3q27-qter), larger cohorts with complete phenotypic characterization will be needed to confirm this correlation.

Pure 3q duplications should be distinguished from complex chromosomal rearrangements involving additional chromosomal imbalances, such as concomitant deletions of 3p [13] or mosaic deletion-duplication syndromes [14]. These complex rearrangements give rise to composite phenotypes that preclude precise genotype-phenotype attribution. In contrast, the present case represents a pure *de novo* 3q26.33-q28 duplication, confirmed by integrated conventional cytogenetic and molecular analyses. This finding provides valuable insight into the specific phenotypic contribution of this genomic region and further strengthens genotype-phenotype correlations for pure 3q duplication syndrome.

The presence of an isolated copy number gain involving a single chromosomal arm, in the absence of additional structural rearrangements, strongly suggests an intrachromosomal

mechanism. Such duplications most likely arise through non-allelic homologous recombination (NAHR) between low-copy repeats (LCRs) or through replication-based mechanisms, including fork stalling and template switching (FoSTeS) or microhomology-mediated break-induced replication (MMBIR) [15, 16]. The absence of additional chromosomal imbalances, as demonstrated by high-resolution chromosomal microarray analysis and confirmed by FISH, supports the hypothesis of an isolated intrachromosomal event rather than an unbalanced translocation inherited from a parental balanced rearrangement. Additionally, the integrity of the terminal end of chromosome 3 was confirmed by FISH using the subtelomeric probe D3S4560, which showed a normal signal pattern on both chromosomes 3, further excluding the possibility of an undetected parental cryptic translocation involving the 3q terminal region.

Furthermore, the tandem configuration confirmed by FISH showing consecutive signals for each probe (RP11-510K16+, RP11-110C15+, RP11-95L3+) provides additional insight into the underlying mutational mechanism. Examination of the genomic architecture at both breakpoint coordinates using the UCSC Genome Browser Segmental Duplications track (genomicSuperDups, GRCh37/hg19) revealed no segmental duplications within a 100 kb window flanking the proximal breakpoint (chr3:179,659,847). At the distal breakpoint (chr3:190,604,567), interchromosomal segmental duplications sharing homology with sequences on chromosomes 2, 19, and 3 were identified; however, these do not constitute the classical flanking intrachromosomal LCR architecture required for NAHR-mediated tandem duplication. The absence of flanking intrachromosomal LCRs at both breakpoints, combined with the non-recurrent and patient-specific nature of this rearrangement, strongly favors replication-based mechanisms, specifically FoSTeS or MMBIR, as the most plausible mutational mechanism underlying this duplication. The normal parental ages (28 and 32 years) fall within the normal reproductive range, suggesting that the duplication most likely arose as a sporadic mutational event during gametogenesis rather than as an age-associated chromosomal instability.

5. Conclusion

This report represents the first documented case of pure 3q duplication since Serra et al.'s comprehensive 2023 review [3]. Our findings refine the critical genomic region for 3q duplication syndrome, demonstrating that the duplication of the 3q26.33-q28 region contributes significantly to the core phenotype.

The phenotypic profile observed in our patient, including severe neurodevelopmental impairment, increased birth weight, and the absence of cardiac malformations, suggests region-specific effects within chromosome 3q. These observations support the hypothesis that distinct subregions of 3q differentially modulate growth, cardiac development, and neurological features, thereby improving genotype-phenotype correlations in pure 3q duplication syndrome.

The tandem configuration and *de novo* origin of the duplication, confirmed through integrated cytogenetic approaches, support an intrachromosomal replication-based mechanism, most consistent with FoSTeS or MMBIR, given the absence of flanking intrachromosomal low-copy repeats at both breakpoints. This case underscores the importance of combining conventional cytogenetics, FISH, and chromosomal microarray analysis for the accurate diagnosis of rare chromosomal disorders.

These findings contribute to refined genetic counseling for affected families and enhance our understanding of dosage-sensitive genes within the 3q region. Future studies integrating

transcriptomic and functional analyses may further clarify the individual contributions of specific genes to the complex phenotype associated with 3q duplication syndrome.

Acknowledgments

We thank the patient and her family.

Author Contributions

HB, NB, ZEA, FO, YD, TL, IMC, LS, and AN planned, performed the experiments, and wrote the manuscript. NB, FO, SCE performed the clinical evaluation. LS, TL, IMC and AN planned, performed the experiments, and revised the manuscript.

Funding

This study had no funding source.

Competing Interests

The authors have no conflicts of interest to declare.

Data Availability Statement

All data generated or analyzed during this study are included in this article.

AI-Assisted Technologies Statement

Artificial intelligence (AI) tools were used solely for basic grammar correction and language refinement in the preparation of this manuscript. Specifically, OpenAI's ChatGPT was employed to improve the readability and linguistic clarity of the English text. All scientific content, data interpretation, and conclusions were developed independently by the author. The authors have thoroughly reviewed and edited the AI-assisted text to ensure its accuracy and accept full responsibility for the content of the manuscript.

References

1. Falek A, Schmidt R, Jervis GA. Familial de Lange syndrome with chromosome abnormalities. Pediatrics. 1966; 37: 92-101.
2. Faas BH, De Vries BB, Van Es-Van Gaal J, Merkx G, Draaisma JM, Smeets DF. A new case of dup(3q) syndrome due to a pure duplication of 3qter. Clin Genet. 2002; 62: 315-320.
3. Serra G, Antona V, Cimador M, Collodoro G, Guida M, Piro E, et al. New insights on partial trisomy 3q syndrome: *De novo* 3q27.1-q29 duplication in a newborn with pre and postnatal overgrowth and assisted reproductive conception. Ital J Pediatr. 2023; 49: 17.
4. Meins M, Hagh JK, Gerresheim F, Einhoff E, Olschewski H, Strehl H, et al. Novel case of dup(3q) syndrome due to a *de novo* interstitial duplication 3q24-q26.31 with minimal overlap to the dup(3q) critical region. Am J Med Genet A. 2005; 132A: 84-89.

5. Wilson GN, Hieber VC, Schmickel RD. The association of chromosome 3 duplication and the Correlia de Lange syndrome. J Pediatr. 1978; 93: 783-788.
6. Ballif BC, Theisen A, Coppinger J, Gowans GC, Hersh JH, Madan-Khetarpal S, et al. Expanding the clinical phenotype of the 3q29 microdeletion syndrome and characterization of the reciprocal microduplication. Mol Cytogenet. 2008; 1: 8.
7. Lisi EC, Hamosh A, Doheny KF, Squibb E, Jackson B, Galczynski R, et al. 3q29 interstitial microduplication: A new syndrome in a three-generation family. Am J Med Genet A. 2008; 146A: 601-609.
8. Azar GM, Conte RA, Kleyman SM, Logush AZ, Verma RS. Probing the human genome in search for a new 3q syndrome. Ann Genet. 1999; 42: 95-100.
9. Pavone P, Praticò AD, Falsaperla R, Ruggieri M, Neri G, Pavone V, et al. A girl with a 14.7 Mb 3q26.32-q28 duplication: A new report of 3q duplication syndrome and a literature review. Clin Dysmorphol. 2016; 25: 121-127.
10. Taşdelen E, İli EG, Altıner Ş, Ceylan AC, Tuncalı T. Genotype phenotype correlation of A case having chromosome 3 imbalance. J Ankara Univ Fac Med. 2021; 74: 365-369.
11. Sowińska-Seidler A, Socha M, Jamsheer A. Split-hand/foot malformation-molecular cause and implications in genetic counseling. J Appl Genet. 2014; 55: 105-115.
12. Collins RL, Glessner JT, Porcu E, Lepamets M, Brandon R, Lauricella C, et al. A cross-disorder dosage sensitivity map of the human genome. Cell. 2022; 185: 3041-3055.e25.
13. Allderdice PW, Browne N, Murphy DP. Chromosome 3 duplication q21 leads to qter deletion p25 leads to pter syndrome in children of carriers of a pericentric inversion inv(3)(p25q21). Am J Hum Genet. 1975; 27: 699-718.
14. Chen CP, Su YN, Hsu CY, Chern SR, Lee CC, Chen YT, et al. Mosaic deletion-duplication syndrome of chromosome 3: Prenatal molecular cytogenetic diagnosis using cultured and uncultured amniocytes and association with fetoplacental discrepancy. Taiwan J Obstet Gynecol. 2011; 50: 485-491.
15. Liu P, Carvalho CM, Hastings PJ, Lupski JR. Mechanisms for recurrent and complex human genomic rearrangements. Curr Opin Genet Dev. 2012; 22: 211-220.
16. Hastings PJ, Lupski JR, Rosenberg SM, Ira G. Mechanisms of change in gene copy number. Nat Rev Genet. 2009; 10: 551-564.